

Durham Research Online

Deposited in DRO:

16 January 2019

Version of attached file:

Accepted Version

Peer-review status of attached file:

Peer-reviewed

Citation for published item:

Treat, C.C. and Kleinen, T. and Broothaerts, N. and Dalton, A.S. and Dommain, R. and Douglas, T.A. and Drexler, J. and Finkelstein, G. and Grosse, G. and Hope, G. and Hutchings, J. and Jones, M.C. and Kuhry, P. and Lacourse, T. and Lähteenoja, O. and Loisel, J. and Notebaert, B. and Payne, R. and Peteet, D. and Sannel, A.B.K. and Stelling, J.M. and Strauss, J. and Swindles, G. and Talbot, J. and Tarnocai, C. and Väiranta, M. and Verstraeten, G. and Williams, C.J. and Xia, Z. and Yu, Z. and Hättestrand, M. and Alexanderson, H. and Brovkin, V. (2019) 'Widespread global peatland establishment and persistence over the last 130,000 y.', *Proceedings of the National Academy of Sciences of the United States of America.*, 116 (11). pp. 4822-4827.

Further information on publisher's website:

<https://doi.org/10.1073/pnas.1813305116>

Publisher's copyright statement:

Copyright 2019 National Academy of Sciences. Users may view, reproduce, or store journal content, provided that the information is only for their personal, noncommercial use.

Additional information:

Use policy

The full-text may be used and/or reproduced, and given to third parties in any format or medium, without prior permission or charge, for personal research or study, educational, or not-for-profit purposes provided that:

- a full bibliographic reference is made to the original source
- a [link](#) is made to the metadata record in DRO
- the full-text is not changed in any way

The full-text must not be sold in any format or medium without the formal permission of the copyright holders.

Please consult the [full DRO policy](#) for further details.

Widespread global peatland establishment and persistence over the last 130,000 years

Claire C. Treat^{1*}, Thomas Kleinen², Nils Broothaerts³, April S. Dalton⁴, René Dommain^{5,6}, Thomas A. Douglas⁷, Judith Drexler⁸, Sarah A. Finkelstein⁴, Guido Grosse^{5,9}, Geoff Hope¹⁰, Jack Hutchings¹¹, Miriam C. Jones¹², Peter Kuhry¹³, Terri Lacourse¹⁴, Outi Lähteenoja¹⁵, Julie Loisel¹⁶, Bastiaan Notebaert³, Richard Payne^{17,18}, Dorothy Peteet¹⁹, A. Britta K. Sannel¹³, Jonathan M. Stelling²⁰, Jens Strauss⁹, Graeme T. Swindles²¹, Julie Talbot²², Charles Tarnocai²³, Minna Väliranta²⁴, Gert Verstraeten³, Christopher J. Williams²⁵, Zhengyu Xia²⁰, Zicheng Yu²⁰, Martina Hättestrand¹³, Helena Alexanderson²⁶, Victor Brovkin²

¹ Department of Environmental and Biological Sciences, University of Eastern Finland, 70211 Kuopio, Finland.

² Max Planck Institute for Meteorology, Bundesstrasse 53, 20146 Hamburg, Germany.

³ Department of Earth and Environmental Sciences, Division of Geography and Tourism, KU Leuven, Celestijnenlaan 200E, B-3001 Belgium.

⁴ Department of Earth Sciences, University of Toronto, Toronto, Ontario, Canada M5S 3B1.

⁵ Institute of Earth and Environmental Science, University of Potsdam, 14476 Potsdam, Germany.

⁶ Department of Anthropology, Smithsonian Institution, National Museum of Natural History, Washington, DC, 20013, USA.

⁷ U.S. Army Cold Regions Research and Engineering Laboratory, Fort Wainwright, Alaska, USA.

⁸ U.S. Geological Survey, California Water Science Center, 6000 J Street, Placer Hall, Sacramento, California, USA.

⁹ Alfred Wegener Institute Helmholtz Centre for Polar and Marine Research, Telegrafenberg A45, 14473 Potsdam, Germany.

¹⁰ College Asia and the Pacific, Australian National University, Canberra ACT, Australia.

¹¹ Department of Geological Sciences, University of Florida, Gainesville, FL, USA.

¹² Eastern Geology and Paleoclimate Science Center, U.S. Geological Survey, Reston, VA, USA.

¹³ Department of Physical Geography, Stockholm University, 10691 Stockholm, Sweden.

¹⁴ Department of Biology, University of Victoria, Victoria, BC, Canada.

¹⁵ School of Life Sciences, Arizona State University, Tempe, AZ, USA.

¹⁶ Department of Geography, Texas A&M University, College Station, TX 77843, USA.

¹⁷ Environment, University of York, York YO105DD, UK.

¹⁸ Department of Zoology and Ecology, Penza State University, Krasnaya str. 40, 440026 Penza, Russia.

¹⁹ NASA GISS, New York, NY 10025, USA.

²⁰ Department of Earth and Environmental Sciences, Lehigh University, Pennsylvania 18015, USA.

²¹ School of Geography, University of Leeds, Leeds, LS2 9JT, UK.

²² Department of Geography, University of Montreal, Montreal, Quebec, Canada.

²³ Research Branch, Agriculture and Agri-Food Canada, Ottawa, Ontario, Canada.

²⁴ Environmental Change Research Unit (ECRU), Ecosystems and Environment Research Programme, University of Helsinki, Helsinki, Finland.

²⁵ Department of Earth and Environment, Franklin and Marshall College, Lancaster, Pennsylvania 17603, USA

²⁶ Department of Geology, Lund University, Lund, Sweden

* Correspondence to: claire.treat@uef.fi

Abstract

Glacial-interglacial variations in CO₂ and methane in polar ice cores have been attributed in part to changes in global wetland extent but the wetland distribution prior to the Last Glacial Maximum (LGM, 21-18 ka) remains virtually unknown. We present the first study of global peatland extent and carbon (C) stocks through the last glacial cycle (130 ka - present) using a newly compiled database of 1063 detailed stratigraphic records of peat deposits buried by mineral sediments as well as a global peatland model. Quantitative agreement between modeling and observations shows extensive peat accumulation prior to the LGM in northern latitudes (>40°N), particularly during warmer periods including the last interglacial (130-116 ka, MIS 5e) and the last interstadial (57-29 ka, MIS 3). During cooling periods of glacial advance and permafrost formation, the burial of northern peatlands by glaciers and mineral sediments decreased active peatland extent, thickness, and modeled C stocks by 70-90% from warmer times. Tropical peatland extent and C stocks show little temporal variation throughout the study period. While the increased burial of northern peats was correlated with cooling periods, the burial of tropical peat was driven by hydrologic changes. These results show that northern peatlands accumulate significant C stocks during warmer times, indicating their potential for C sequestration during the warming Anthropocene, while the burial of peats represents a mechanism for long-term terrestrial C storage in the earth system.

Significance statement

During the Holocene (11,600 years ago – present), northern peatlands accumulated significant C stocks over millennia. However, virtually nothing is known about peatlands that are no longer in the landscape, including ones formed prior to the Holocene: where were they, when did they form, why did they disappear? We used records of peatlands buried by mineral sediments for the

first-ever reconstruction of peat-forming wetlands for the past 130,000 years. Northern peatlands expanded across high latitudes during warm periods and were buried during periods of glacial advance in northern latitudes. Thus, peat accumulation and burial represent a key long-term C storage mechanism in the earth system.

Introduction

The distribution of carbon stocks during glacial cycles represents a key uncertainty in the long-term global C budget and the global climate system (1, 2). During the last glaciation, ice core records show low atmospheric CO₂ concentrations and a strong increase following deglaciation, correlating with temperature increases. However, the mechanisms behind these observations are still unknown; hypotheses include both marine (1) and terrestrial processes (2, 3). At present, northern peatlands, wetlands with thick (>30-40 cm) organic sediments, contain an estimated 400 - 500 Pg C (4, 5) and tropical peatlands contain an estimated ~105 Pg C (4, 6). These peatlands have sequestered atmospheric CO₂ over millennia because plant productivity exceeds decomposition, which is slowed by the saturated and anoxic soil conditions found in these wetlands and leads to the accumulation of undecomposed organic matter (peat). As the largest natural source of methane (CH₄) to the atmosphere (7), tropical and high-latitude wetland emissions are often invoked to explain variations in atmospheric CH₄ concentrations over glacial cycles (8, 9) and abrupt CH₄ increases during periods of rapid climatic change (9, 10).

Beyond CH₄ emissions, the role of peatlands in the global C cycle on glacial-interglacial time scales has not been considered due to a lack of systematic evidence of peatland extent prior to the last glacial maximum (LGM, 21-18 ka; Fig. 1). Previous studies have explored the timing and locations of peatland formation (or “peat initiation”) and expansion in northern high latitudes

during the Holocene (from 11.6 ka to the pre-industrial period) using basal ages, the oldest age of the deepest sediments found in present-day peatlands. These studies have shown that most peatlands formed following the LGM (10-14). On the other hand, large coal deposits from times as old as the Carboniferous period (359 – 299 Ma) and as young as the Miocene (23-5 Ma) indicate that significant peat accumulated prior to the Holocene. Despite modeling studies showing the likely importance of a peatland C pool in the global C cycle (15, 16), there is little evidence of peat prior to the Holocene other than ancient coal deposits.

Here, we identify the spatial and temporal distribution of ancient peatlands preserved by burial under minerogenic sediments (“buried peat deposits”) and model peatland C stocks for the past 130,000 years (130 ka) to test the response of peatland C stocks to the highly variable climate conditions prior to the Holocene. We create a new dataset of buried peat deposits that includes 1063 profiles globally (Fig. 1), including 37 previously unpublished profiles, by synthesizing sediment exposures, and soil, lake, and marine cores containing peat sections (Methods, Data S1). In addition to location, we use several attributes of the buried peat deposits in our analysis: 1) the timing of active peat accumulation when sites were actively accumulating peat (determined from sediment dating methods) as opposed to being buried or otherwise inactive; 2) the number of sites that were actively accumulating peat at the same time (active buried sites, a count) which is a proxy for peatland extent; 3) the thickness of these buried peat deposits, which is a proxy for the total C stock of the peat deposits that accumulated during the period of active deposition (thickness, when reported). We model peatland C stocks from 126 ka to the preindustrial (1850 CE) using the peatland-enabled CLIMBER2-LPJ model (17), one of the few global earth system models to simulate dynamic wetland area and peat thickness (Methods).

Results and Discussion

Spatial and temporal distribution of peats in the northern region (>40°N)

There is substantial evidence for widespread northern peatlands from more than 40 sites during the last interglacial (130 – 116 ka, MIS 5e), when continental ice sheets were largely absent in the northern hemisphere (Fig. 2d, S1). During a period of cooling during MIS 4 (~71-57 ka BP, Fig. 2b), northern buried peat records decreased by 75% to the smallest number outside of the LGM (Fig. 2d, Table 1, Fig. S1). As temperatures increased during the MIS 3 interstadial, the number of northern buried peat records increased six-fold, particularly between 57 - 45 ka (Fig. 2d, Table 1). Peatland expansion continued between 35 - 29 ka with peat formation in the northern coastal lowlands of Siberia, Alaska and Beringia, and central North America (Fig. S1).

After 29 ka, the number of active northern peat deposits decreased by >80% (Fig. 2d, Table 1), coinciding with a cooling trend in Northern Hemisphere temperature (Fig. 2a, 2b), the expansion of glaciers and ice sheets (Fig. 2a), and the burial of peat by glacial sediments. Even in non-glaciated regions of Siberia, Alaska, and the Southeastern US, active peatland extent was greatly reduced (Table 1; Fig. S1) as peats not covered by glacial sediments were buried by aeolian deposits (27%), coastal sediments (30%), and permafrost-associated processes (16%). The number of active northern peat deposits reached a minimum during the LGM (Table 1, Fig. 2d) as temperatures reached their minimum (Fig. 2b) and ice extent reached its maximum (Fig. 2a). Eighty percent of the remaining peat records at the LGM were found in present-day coastal zones, while limited peatland formation also occurred at the southern margin of glaciated regions (Fig. S1).

As glacial retreat began after 18 ka, peatlands expanded northward in newly exposed lowland areas along the southern ice margins of the Laurentide and Scandinavian ice sheets, forming both now-buried peats and present-day peatlands (Table 2, Fig. 2d, Fig. S2). The rapid establishment of northern peatlands occurred during the first half of the Holocene (Table 2) as peat accumulated in the West Siberian Lowlands, Fennoscandia, and Western Canada. The deposition of now-buried peats also increased significantly following the onset of the Holocene, but decreased after 5 ka (Table 2, Fig. 2d) as coastal areas flooded (52% of sites) or hydrological conditions changed (30% of sites).

Modeled northern peatland C stocks agreed well with observations of active peat accumulation in now-buried peat deposits prior to the LGM (Table 1; $\rho=0.77$). During MIS 5e, the maximum modeled active northern peatland C stocks were 340 Pg at 120 ka, corresponding to the largest number of northern sites with active peat deposition prior to the LGM (Fig. 2d). During MIS 4, modeled active peatland C stocks decreased to 210 Pg C, corresponding to a decrease in peatland extent, here evidenced by the number of sites with active peat deposition (Table 1). During warmer MIS 3, modeled active peatland stocks again increased to 265 Pg C, corresponding with a significant increase in peatland extent (Table 1). As glaciers expanded during MIS 2 and into the LGM, modeled active peatland C stocks decreased by 70% from MIS 3 values to a minimum of ~80 Pg C. During this period, active peatland extent decreased significantly as peats were buried by glacial sediments and other sediment types; observations show that the remaining peats were shallower (Table 1).

Following the LGM, modeled active peatland C stocks increased slowly prior to the Holocene, adding ~ 60 Pg C, which correlates well with the slow increase in active peatland formation observed during this period (Table 2). During the beginning of the Holocene, modeled

active peatland C stocks increased rapidly, corresponding to the strong increase in observed peatland initiation (Table 2, Fig. 2e, $r = 0.99$). A significant number (33%) of present-day peatlands were formed after 5 ka (Table 2, Fig. 2e) and modeled active peatland C stocks increased by approximately the same amount (34%) during this period. Modeled active northern peatland C stocks reached a maximum of 410 Pg C in the pre-industrial period (315 – 590 Pg C; Table 2), an increase of 330 Pg C since the LGM.

Spatial and temporal distribution of peats in the tropics (30°N – 30°S)

The first known buried peat deposit from the tropics formed between 164 – 122 ka (18) in New Guinea, followed by a hiatus with no evidence of tropical peat deposition until 60 ka (Fig. 2f, Fig. S3). The first evidence of peatland establishment in equatorial and southern Africa dates to 50 – 45 ka (Fig. S3); the majority of sites from that time persist to the present day (Fig. S3, Data S2). The number of actively accumulating peats in the tropics increased after 45 ka, then decreased during MIS 2 through the LGM as peats were buried by fluvial and coastal processes (Table S1, Data S1). However, the formation of new peatlands resulted in little apparent change in tropical peatland distribution (Fig. S3).

As global temperatures increased after the LGM and into the Bølling-Allerød, the rate of peatland initiation increased after ~15 ka for both buried and present-day tropical peatlands (Table 2; Fig. 2g) as peats accumulated on the then-exposed continental shelves in Indonesia and western Africa (Fig. S4). The number of active tropical peat records decreased and peat initiation slowed between the Bølling-Allerød and the early Holocene (Fig. 2f, Table 2) as continental shelves flooded and buried coastal sites in Southeast Asia, including sites in the Strait of Malacca, Thailand coast, and Java Sea (Fig. S4). As the sea level stabilized (19), the number of

now-buried tropical peat records in Southeast Asia more than doubled during the mid-Holocene between 8.2 ka and 5 ka (Fig. 2f, Table 2, Fig. S4) as peatlands expanded across Indonesia and Malaysia (Fig. 2g, Table 2, Fig. S4). While the areas of active tropical peatland formation shifted in space and time (Fig. S3, S4), the total modeled active tropical peatland C stocks remained relatively constant throughout the interglacial at an estimated 145 Pg C (80-215 Pg C; Table S1).

Factors controlling the distribution of peat in space and time

Peat accumulation occurs when vegetation productivity exceeds decomposition losses and is facilitated by anoxic conditions due to poor drainage in wetlands. Understanding the drivers of peat accumulation and loss under a broad range of climatic conditions can ultimately improve projections of the response of peatland C stocks to future climatic changes (20) through improved representation of processes controlling peat accumulation. Process-based modeling approaches have predicted a wide range of outcomes in response to future climate change, from substantial loss of peat due to drying (21) and permafrost thaw (22) to continued peat accumulation (23). These data show another possible fate for peat: burial.

Our results show that warm periods with higher precipitation (e.g. MIS 5e, MIS 3 (57 – 29 ka), Holocene) corresponded to a higher occurrence of northern peat deposition and greater northern peatland C stocks, evidenced by the observed number of sites, observed peat thickness, and modeled C stocks (Table 1, Figs. 2b, 2d, 2e). Whether increased peat formation during warm periods was caused by changes in productivity and decomposition rates or other factors such as increases in area is unclear. A recent analysis suggests that the number of growing degree days is the key driver of northern peatland formation in ice-free areas during the Holocene (14). However, higher temperatures also correlate with smaller areal extent of ice sheets and glaciated

areas (Figs. 2a, 2b), potentially exposing relatively flat, vegetation-free terrain and alleviating a spatial bottleneck for peatland formation (11). Peat formation on formerly glaciated and ice sheet areas was responsible for ~30% of the modeled increase in peatland areas between the LGM and the pre-industrial Holocene (Table S2). Regardless, net peat accumulation will likely continue with warming as long as disturbances such as wildfire, drainage, or flooding are not significant (20).

Northern peatland extent and C stocks were smallest during cold, dry periods with enhanced glaciation (e.g. MIS 4 and 2, or 71 – 57 ka and 29 – 21 ka, respectively; Table 1, Fig. 2, Fig. S1). Colder periods may not have directly resulted in the loss of peat (e.g. to the atmosphere), but instead favored processes (aeolian, glacial, and glaciofluvial) that resulted in rapid mineral deposition and subsequent peat burial while limiting new peatland development or recovery of peat accumulation due to dry or continental conditions (24). While limited observational evidence of peats during these cold periods does not mean peatlands were absent, the persistence of peat deposits from older, warmer periods (MIS 3, MIS 5e, Fig. 2d) indicates this trend of increased peat formation during warmer times and burial during colder periods is robust.

During warm periods (the Holocene) and in warm locations (the tropics), peat burial was related to other factors than temperature. Tropical peatland deposition was relatively insensitive to global temperature fluctuations, as evidenced by their persistent presence on the landscape after 50 ka during a range of climatic conditions in both data and model results (Fig. 2f, Table 2, Table S1). Instead, tropical peat formation responded mainly to changing hydrologic conditions. For example, approximately one-third of the tropical buried peats that formed during the Holocene were buried as sea level rose (15/46 sites), while others were formed as rising sea level

altered regional hydrology in coastal regions (14, 19). Hydrological changes were responsible for the cessation of peat accumulation at approximately one-third of now-buried tropical peatland sites during the Holocene (14/46 sites) as water tables in lakes and wetlands both rose and fell. Similar patterns were observed for northern peats after 5 ka, when coastal flooding and changing hydrology buried >80% of the buried peat sites. Additionally, anthropogenic influence was important for the burial of tropical peatlands (9/46 sites) and some northern peatlands (2/41 sites) during the Holocene (25). The burial and destruction of peats in Central America, New Guinea, and Borneo has been attributed to a combination of changes in agricultural practices, deforestation, and changing environmental conditions (26). In Western and Central Europe, anthropogenic factors such as changing agricultural practices, deforestation, and subsequent changes in hydrology and soil erosion led to an increase in floodplain sedimentation and peat burial (27) in many peat-forming wetlands located in floodplains.

Implications for the global C budget

While the importance of northern peatland expansion for global C cycles during the Holocene has been previously recognized (2, 4, 15, 28), these new results show the importance of both tropical and northern peatlands to the global C cycle during and prior to the Holocene. The accumulation of 560 Pg C in peatlands globally comprises between 18 and 25% of the total land C modelled by LPJ for the pre-industrial Holocene and represents a significant C storage term in the earth system. From LGM to pre-industrial, the global peatland C stock increased by 300 Pg C, in agreement with previous estimates of significant increases in histosol C storage from LGM to the present (3, 29). The increase in peatland C was substantially larger than the 190 PgC increase in the atmospheric CO₂ inventory between LGM and pre-industrial. To balance

the global C budget for the LGM to pre-industrial, the remainder of the C budget change must have been supplied by the other C pools, likely the ocean.

Previously, it has been assumed that the loss of peatlands meant increased decomposition and the release of peatland C to the atmosphere (21, 30) but these data demonstrate otherwise. With burial by mineral sediments, peat C can be incorporated into long-term storage in soil C stocks, as evidenced by the age of these deposits (Fig. 1, 2, S1). While decomposition of buried peat may occur, it may also be limited by factors affecting decomposition rates in deep soils and sub-glacial sediments: anoxia resulting from slow rates of oxygen diffusion or saturation (31), limited microbial activity at depth (32), and cold temperatures or permafrost (33), which was frequently observed in these data (Table S1). Peat accumulation and subsequent burial by mineral sediments provides a mechanism for the transfer of atmospheric CO₂ to a stable terrestrial C pool, where it can be preserved for millennia or longer despite decreases in active peatland area and C stocks (Fig. 2, Table 1).

Peatland C accumulation and burial has potential implications for the re-distribution of C among global reservoirs at glacial/interglacial timescales, which has been a longstanding debate (1, 2). Proposed mechanisms for CO₂ sequestration during the LGM include enhanced CO₂ storage in deep oceans (1) or formation of inactive terrestrial C stocks (2), such as C buried by glacial sediments (34) or permafrost soils (2, 3, 28, 35). Our observational data demonstrate that peat burial by glacial sediments and other depositional processes was widespread during the glacial expansion preceding the LGM (Figure 2d, Table 1) and provide an alternative explanation for the incorporation of significant amounts of organic matter into long-term soil C stocks and permafrost prior to the LGM (2, 3). Our modeling results can be used to estimate the upper bounds of peat C burial from the loss of active peatland C stocks between MIS 3 and LGM,

assuming all peat was buried rather than lost to the atmosphere. These model results show maximum total global peatland C stocks of 433 PgC and 260 PgC for MIS 3 and LGM, respectively, a decrease of 170 PgC in active peatland C stocks. The loss of active peat C is substantially larger than the ~30 PgC decrease in the atmospheric CO₂ inventory during this period. To balance the global C budget for MIS 3 to LGM, the remainder of the C budget change must to have been taken up by the other C pools, likely the ocean. In the scenario of complete peat C burial rather than loss to the atmosphere, a buried peat C stock of 170 Pg C requires less C uptake by the ocean and other pools. However, this buried stock is substantially smaller than the 700 Pg C increase in inert land carbon at LGM compared to the present hypothesized by Ciais, *et al.* (2), thus requiring substantial contributions from other processes. Further field data and modeling investigations will be required to better constrain the size of both buried peat C pools and terrestrial C pools during this transitional period.

While previous modeling results suggested that C sequestration in peatlands was a key process regulating atmospheric CO₂ concentrations during past interglacial periods (15), these new observations of buried peats demonstrate that peatlands have been an important C stock since the last interglacial (Table 1). In particular, actively forming northern peatlands both accumulated C and emitted CH₄ during warm periods. During colder periods of glacial advance, the burial of significant northern peat C stocks by mineral sediments and formation of permafrost would have all but stopped decomposition and CH₄ emissions (36), resulting in the long-term burial of peatland C. The widespread distribution of buried peats and the large magnitude of the change in peatland C stock throughout the last glacial cycle suggests that peat formation during warmer times and burial during colder periods has a significant impact on the global carbon cycle that has not been previously quantified (2).

Materials and Methods

Buried peat dataset

We compiled 1063 records of buried peat layers from peats overlain by minerogenic sediments described in the published literature and from 37 unpublished profiles (Fig. 1, Data S1). We identified profiles based on author knowledge, solicitations through existing research networks, and literature searches on Web of Knowledge and Google Scholar using the terms “buried peat”, “buried peat deposits”, “histic paleosols”, “organic paleosols”, “interglacial peat”, “MIS 5 and peat”, “MIS 3 and peat”. We defined peat broadly as organic-rich sediment derived from wetland or limnic environments deposited in-situ or within the local catchment. We extracted information on the profile location, depth of the organic-rich sediments, the timing of deposition (when available), the depositional environment of the organic-rich sediment (alluvial, limnic, wetland, upland), the type and origin of the overlying sediments, and other site descriptors. The dataset is publicly available via the PANGAEA data archive (doi:10.1594/PANGAEA.873066).

Chronological control for the timing of peat formation was available for 930 profiles (88% of samples) and was based mainly on calibrated radiocarbon dates for 786 profiles younger than 50 ka (alternative dating was used for 18 profiles). For profiles older than 50 ka, chronologies were based on tephrochronology (14 profiles), optically or thermally stimulated luminescence dating (OSL/TL; 6 profiles), stratigraphic position relative to tills and other sediment types of known depositional age (25 profiles, plus 19 profiles with infinite radiocarbon dates), pollen (11 profiles), or Uranium-Thorium dating (8 profiles). Multiple dating proxies were used at 41 profiles. Many of the buried peat sites compiled for this study are

chronologically constrained by radiocarbon dating, which imposes some important considerations onto our dataset. Notably, the apparent increase in the number of buried peat sites after 50 ka (Fig. 2d, 2f) is likely related to the technical limitations of radiocarbon dating because deposits <50 ka are more readily ‘datable’ than older deposits. Other potential errors in the chronological control of this study include contamination by modern radiocarbon, ancient radiocarbon, and/or poor chronological constraints due to having only one date from within the buried peat section or proximate sediment layers (683 of 930 dated deposits) or lack of suitable materials for various dating approaches. Ideally, additional dating of buried peat sections would constrain the duration of peat persistence on the landscape and clarify the timing of peat development in relation to atmospheric CO₂ and CH₄ records.

We used peatland basal ages (oldest date from present-day peatlands, indicating the beginning of peat accumulation) to place the development of the buried peats in the context of the development of present-day peatlands. The peatland initiation dataset consisted of 3942 basal ages and was based on a compilation of several existing basal age datasets for northern peatlands (10, 12, 13, 37), tropical peatlands (4, 19), and 473 additional basal ages from newer literature not included in previous compilations (Data S2). The peatland initiation dataset is archived and publically available (doi: 10.1594/PANGAEA.873065).

All radiocarbon ages were calibrated with IntCal13 (38) and all ages referred to in the text have been calibrated (cal BP). If errors on the radiocarbon ages were not reported, we assumed a 10% error. Calibrated dates were rounded to the nearest decade. In order to assess the uncertainties associated with the core chronologies, we used bootstrap resampling (n=1000) to develop an uncertainty distribution based on the chronologic uncertainty. For each statistical replicate, all buried peats samples were assigned ages based on randomly sampled values that

fell within the maximum and minimum calibrated ages (including 2-sigma age uncertainty) for each deposit (r command: sample). A similar procedure was used for assessing error in peatland initiation dates. Calibrated peatland basal ages were assigned an age based on a randomly sampled value that fell within the 2-sigma range of the calibrated basal peat date; peat was assumed to occur thereafter. These resampling procedures were repeated 1000 times for each analysis (northern buried peats, northern peat initiation, tropical buried peats, tropical peatland initiation); the mean and 95% confidence intervals of the statistical replicates are shown. Profiles without chronological control (133 of 1063 profiles) remain in the database (Fig. 1) but could not be used to track peat C persistence over the last glacial cycle (Fig. 2d, 2f). For comparison between peat records and climate (Fig. 2), we used the harmonized $\delta^{18}\text{O}$ records (39), and the results of the CLIMBER2 earth system model simulations through the last glacial cycle (40).

We performed a transient model experiment using a climate-carbon cycle model, an updated version of the peatland-enabled CLIMBER2-LPJ model (17) in order to determine peatland extent and C stocks through the last glacial cycle because these could not be interpreted from the observations (Supplemental Information). Briefly, CLIMBER2-LPJ consists of the dynamic Global Vegetation Model LPJ (41), coupled to the Earth System Model of Intermediate Complexity CLIMBER2 (42). LPJ is run on a $0.5^\circ \times 0.5^\circ$ grid and is coupled to the coarser grid of CLIMBER2 via climatic anomalies and carbon fluxes (17, 43). Ice sheet areas, as well as sea level and isostasy, are prescribed from an experiment with an ice-sheet enabled version of the CLIMBER2 model (44). The global peatland model determines peatland location and extent from a combination of topography and grid-cell scale water balance using a TOPMODEL approach as described in Kleinen, Brovkin and Schuldt (17), as opposed to being prescribed, as in other global model simulations of Holocene peatlands (23). This allows peatland areas to form

dynamically in response to changing hydrologic conditions. Sea level is dynamic in this model framework, allowing us to estimate peatland areas on exposed continental shelves. The peatland model was driven with orbital changes, CO₂ concentrations derived from ice-core data, and ice sheet extent determined using an ice-sheet enabled version of the CLIMBER2 model (44). The model was initialized with a 5000-year spinup period under early Eemian boundary conditions at 126 ka BP and subsequently run transiently from 126 ka BP until 0 BP. Further details about model parameterization and evaluation can be found in the Supplemental Information.

Acknowledgements

This work is the result of a PAGES C-PEAT working group. We thank S. Frolking for helpful discussion. CT was supported by the Max Planck Institute for Meteorology, NSF ARC-1304823, and the Academy of Finland. TK was supported by the German Ministry of Education and Research, BMBF Grants No. 03G0836C and 01LP1507B. TAD was supported by the U.S. Army Engineer Research and Development Center's Basic Research (6.1) Program and the Strategic Environmental Research and Development Program. SAF, TL, and JT were supported by the NSERC of Canada. GG and JS were supported by ERC #338335 and HGF ERC-0013. MJ was supported by USGS Climate and Land Use Change R&D and NSF ARC-1304823. JMS, ZX and ZY were supported by NSF. RJP was supported by the Russian Science Foundation (14-14-00891). Any use of trade, product, or firm names is for descriptive purposes only and does not imply endorsement by the U.S. government.

Author contributions: All authors contributed to data collection and manuscript writing. C.T. led data collection, analysis, and writing. T.K. led model analysis. V.B., G.G., and M.J. contributed to analysis.

References

1. Sigman DM, Hain MP, & Haug GH (2010) The polar ocean and glacial cycles in atmospheric CO₂ concentration. *Nature* 466:47.
2. Ciais P, *et al.* (2012) Large inert carbon pool in the terrestrial biosphere during the Last Glacial Maximum. *Nature Geoscience* 5(1):74.
3. Lindgren A, Hugelius G, & Kuhry P (2018) Extensive loss of past permafrost carbon but a net accumulation into present-day soils. *Nature* 560(7717):219-222.
4. Yu Z, Loisel J, Brosseau DP, Beilman DW, & Hunt SJ (2010) Global peatland dynamics since the Last Glacial Maximum. *Geophys. Res. Lett.* 37(13):L13402.
5. Gorham E (1991) Northern Peatlands - Role in the Carbon-Cycle and Probable Responses to Climatic Warming. *Ecological Applications* 1(2):182-195.
6. Dargie GC, *et al.* (2017) Age, extent and carbon storage of the central Congo Basin peatland complex. *Nature* 542(542):96-90.
7. Saunois M, *et al.* (2016) The global methane budget 2000-2012. *Earth System Science Data* 8(2):697.
8. Spahni R, *et al.* (2005) Atmospheric Methane and Nitrous Oxide of the Late Pleistocene from Antarctic Ice Cores. *Science* 310(5752):1317-1321.
9. Loulergue L, *et al.* (2008) Orbital and millennial-scale features of atmospheric CH₄ over the past 800,000 years. *Nature* 453(7193):383-386.
10. MacDonald GM, *et al.* (2006) Rapid early development of circumarctic peatlands and atmospheric CH₄ and CO₂ variations. *Science* 314(5797):285-288.
11. Gorham E, Lehman C, Dyke A, Janssens J, & Dyke L (2007) Temporal and spatial aspects of peatland initiation following deglaciation in North America. *Quaternary Science Reviews* 26(3-4):300-311.
12. Jones MC & Yu Z (2010) Rapid deglacial and early Holocene expansion of peatlands in Alaska. *Proceedings of the National Academy of Sciences* 107(16):7347-7352.
13. Korhola A, *et al.* (2010) The importance of northern peatland expansion to the late-Holocene rise of atmospheric methane. *Quaternary Science Reviews* 29(5-6):611-617.
14. Morris PJ, *et al.* (2018) Global peatland initiation driven by regionally asynchronous warming. *Proceedings of the National Academy of Sciences* 115(19):4851.
15. Kleinen T, Brovkin V, & Munhoven G (2016) Modelled interglacial carbon cycle dynamics during the Holocene, the Eemian and Marine Isotope Stage (MIS) 11. *Clim. Past* 12(12):2145-2160.
16. DeConto RM, *et al.* (2012) Past extreme warming events linked to massive carbon release from thawing permafrost. *Nature* 484(7392):87-91.
17. Kleinen T, Brovkin V, & Schuldt RJ (2012) A dynamic model of wetland extent and peat accumulation: results for the Holocene. *Biogeosciences* 9(1):235-248.

18. Haberle SG (1998) Late Quaternary vegetation change in the Tari Basin, Papua New Guinea. *Palaeogeography, Palaeoclimatology, Palaeoecology* 137(1):1-24.
19. Dommain R, Couwenberg J, & Joosten H (2011) Development and carbon sequestration of tropical peat domes in south-east Asia: links to post-glacial sea-level changes and Holocene climate variability. *Quaternary Science Reviews* 30(7–8):999-1010.
20. Frolking S, *et al.* (2011) Peatlands in the Earth's 21st century climate systems. *Environmental Reviews* 19:371-396.
21. Ise T, Dunn AL, Wofsy SC, & Moorcroft PR (2008) High sensitivity of peat decomposition to climate change through water-table feedback. *Nature Geosci* 1(11):763-766.
22. Avis CA, Weaver AJ, & Meissner KJ (2011) Reduction in areal extent of high-latitude wetlands in response to permafrost thaw. *Nature Geosci* 4(7):444-448.
23. Spahni R, Joos F, Stocker BD, Steinacher M, & Yu ZC (2013) Transient simulations of the carbon and nitrogen dynamics in northern peatlands: from the Last Glacial Maximum to the 21st century. *Clim. Past* 9(3):1287-1308.
24. Alexandrov GA, Brovkin VA, & Kleinen T (2016) The influence of climate on peatland extent in Western Siberia since the Last Glacial Maximum. *Scientific Reports* 6:24784.
25. Joosten H & Clarke D (2002) *Wise use of mires and peatlands* (International mire conservation group).
26. Haberle SG, Hope GS, & DeFretes Y (1991) Environmental Change in the Baliem Valley, Montane Irian Jaya, Republic of Indonesia. *Journal of Biogeography* 18(1):25-40.
27. Broothaerts N, *et al.* (2014) Non-uniform and diachronous Holocene floodplain evolution: a case study from the Dijle catchment, Belgium. *Journal of Quaternary Science* 29(4):351-360.
28. Crichton KA, Bouttes N, Roche DM, Chappellaz J, & Krinner G (2016) Permafrost carbon as a missing link to explain CO₂ changes during the last deglaciation. *Nature Geoscience* 9:683.
29. Harden JW, Sundquist ET, Stallard RF, & Mark RK (1992) Dynamics of Soil Carbon During Deglaciation of the Laurentide Ice-Sheet. *Science* 258(5090):1921-1924.
30. Yu Z, *et al.* (2011) Peatlands and Their Role in the Global Carbon Cycle. *Eos, Transactions American Geophysical Union* 92(12):97-98.
31. Keiluweit M, Nico PS, Kleber M, & Fendorf S (2016) Are oxygen limitations under recognized regulators of organic carbon turnover in upland soils? *Biogeochemistry* 127(2):157-171.
32. Rumpel C & Koegel-Knabner I (2011) Deep soil organic matter—a key but poorly understood component of terrestrial C cycle. *Plant and Soil* 338(1-2):143-158.
33. Davidson EA & Janssens IA (2006) Temperature sensitivity of soil carbon decomposition and feedbacks to climate change. *Nature* 440(7081):165-173.
34. Zeng N (2003) Glacial-interglacial atmospheric CO₂ change—The glacial burial hypothesis. *Advances in Atmospheric Sciences* 20(5):677-693.
35. Zech R (2012) A permafrost glacial hypothesis—Permafrost carbon might help explaining the Pleistocene ice ages. *Eiszeitalter und Gegenwart E&G/Quaternary science journal* 61(1):84-92.
36. Treat CC, *et al.* (2014) Temperature and peat type control CO₂ and CH₄ production in Alaskan permafrost peats. *Global Change Biology* 20(8):2674–2686.

- 474 37. Packalen MS, Finkelstein SA, & McLaughlin JW (2014) Carbon storage and potential
475 methane production in the Hudson Bay Lowlands since mid-Holocene peat initiation. *Nat*
476 *Commun* 5.
- 477 38. Reimer PJ, *et al.* (2013) IntCal13 and Marine13 Radiocarbon Age Calibration Curves 0–
478 50,000 Years cal BP. *Radiocarbon* 55(4):1869-1887.
- 479 39. Lisiecki LE & Raymo ME (2005) A Pliocene-Pleistocene stack of 57 globally distributed
480 benthic $\delta^{18}\text{O}$ records. *Paleoceanography* 20(1):n/a-n/a.
- 481 40. Ganopolski A & Brovkin V (2017) Simulation of climate, ice sheets and CO₂ evolution
482 during the last four glacial cycles with an Earth system model of intermediate
483 complexity. *Clim. Past* 13(12):1695-1716.
- 484 41. Sitch S, *et al.* (2003) Evaluation of ecosystem dynamics, plant geography and terrestrial
485 carbon cycling in the LPJ dynamic global vegetation model. *Global Change Biology*
486 9(2):161-185.
- 487 42. Petoukhov V, *et al.* (2000) CLIMBER-2: a climate system model of intermediate
488 complexity. Part I: model description and performance for present climate. *Climate*
489 *dynamics* 16(1):1-17.
- 490 43. Kleinen T, Brovkin V, von Bloh W, Archer D, & Munhoven G (2010) Holocene carbon
491 cycle dynamics. *Geophysical Research Letters* 37(2).
- 492 44. Ganopolski A, Calov R, & Claussen M (2010) Simulation of the last glacial cycle with a
493 coupled climate ice-sheet model of intermediate complexity. *Clim Past* 6(2):229-244.
- 494 45. Ehlers J & Gibbard P (2004) Quaternary Glaciations—Extent and Chronology. Vol. 1.
495 *Europe. Elsevier, Amsterdam.*
- 496 46. Fairbanks RG (1989) A 17,000-year glacio-eustatic sea-level record- Influence of glacial
497 melting rates on the Younger Dryas event and deep-ocean circulation. *Nature*
498 342(6250):637-642.
- 499 33. A. Korhola *et al.*, The importance of northern peatland expansion to the late-Holocene
500 rise of atmospheric methane. *Quaternary Science Reviews* 29, 611-617 (2010).
- 501 34. M. C. Jones, Z. Yu, Rapid deglacial and early Holocene expansion of peatlands in
502 Alaska. *Proceedings of the National Academy of Sciences* 107, 7347-7352 (2010).
- 503 35. M. S. Packalen, S. A. Finkelstein, J. W. McLaughlin, Carbon storage and potential
504 methane production in the Hudson Bay Lowlands since mid-Holocene peat initiation. *Nat*
505 *Commun* 5, (2014).
- 506 36. P. J. Reimer *et al.*, IntCal13 and Marine13 Radiocarbon Age Calibration Curves 0–
507 50,000 Years cal BP. *Radiocarbon* 55, 1869-1887 (2013).
- 508 37. S. Frolking, J. Talbot, Z. M. Subin, Exploring the relationship between peatland net
509 carbon balance and apparent carbon accumulation rate at century to millennial time
510 scales. *The Holocene*, (2014).
- 511 38. S. S. Staff, "Soil taxonomy: A basic system of soil classification for making and
512 interpreting soil surveys," *U.S. Department of Agriculture Handbook* (1999).
- 513 39. J. Brigham-Grette, in *Late Cenozoic History of the Interior Basins of Alaska and the*
514 *Yukon*, L. D. Carter, T. D. Hamilton, J. P. Galloway, Eds. (U.S. Geological Survey,
515 Anchorage, 1989), vol. 1026, pp. 107.
- 516 40. S. Sitch *et al.*, Evaluation of ecosystem dynamics, plant geography and terrestrial carbon
517 cycling in the LPJ dynamic global vegetation model. *Global Change Biology* 9, 161-185
518 (2003).

41. V. Petoukhov *et al.*, CLIMBER-2: a climate system model of intermediate complexity. Part I: model description and performance for present climate. *Climate dynamics* **16**, 1-17 (2000).
42. T. Kleinen, V. Brovkin, W. von Bloh, D. Archer, G. Munhoven, Holocene carbon cycle dynamics. *Geophysical Research Letters* **37**, (2010).
43. A. Ganopolski, R. Calov, M. Claussen, Simulation of the last glacial cycle with a coupled climate ice-sheet model of intermediate complexity. *Clim Past* **6**, 229-244 (2010).
44. J. Xu, P. J. Morris, J. Liu, J. Holden, PEATMAP: Refining estimates of global peatland distribution based on a meta-analysis. *CATENA* **160**, 134-140 (2018).
45. E. J. Brook, S. Harder, J. Severinghaus, E. J. Steig, C. M. Sucher, On the origin and timing of rapid changes in atmospheric methane during the Last Glacial Period. *Global Biogeochemical Cycles* **14**, 559-572 (2000).
46. J. Loisel *et al.*, A database and synthesis of northern peatland soil properties and Holocene carbon and nitrogen accumulation. *The Holocene* **24**, 1028-1042 (2014).
47. B. Lehner, P. Döll, Development and validation of a global database of lakes, reservoirs and wetlands. *Journal of Hydrology* **296**, 1-22 (2004).
48. S. E. Page, J. O. Rieley, C. J. Banks, Global and regional importance of the tropical peatland carbon pool. *Global Change Biology* **17**, 798-818 (2011).
49. T. Gumbrecht *et al.*, An expert system model for mapping tropical wetlands and peatlands reveals South America as the largest contributor. *Global Change Biology* **23**, 3581-3599 (2017).

Figure legends

Figure 1. Locations of buried peat and present-day peatland sites. Symbols: Buried peat profiles from the LGM (18 ka) and before (orange circles), post-LGM (yellow circles), and profiles without chronological control (black crosses), and basal ages from present-day peatlands (purple). Laurentide and Scandinavian ice sheet extent shown by white area with dashed border (45), exposed continental shelf areas during the LGM (yellow) based on Etopo DEM + Bathymetry using a -125m sea level (46). Overlapping crosses and circles indicate multiple profiles at site, with and without chronological control.

Figure 2. Climate boundary conditions and peat formation records for northern ($>40^{\circ}\text{N}$) and tropical ($30^{\circ}\text{N} - 30^{\circ}\text{S}$) peatlands for the last 130 ka. Top: Corresponding names for chronostratigraphic units used in the text including the Holocene (HOL), a) LR04 $\delta^{18}\text{O}$ stack (39); b) simulated mean annual temperature for global land areas (40); c) simulated annual precipitation for global land areas (40); d) number of active northern peat deposits now buried (count); e) northern peatland initiation (count); f) number of active peat deposits (now buried) in tropical regions (count); g) tropical peatland initiation (count).

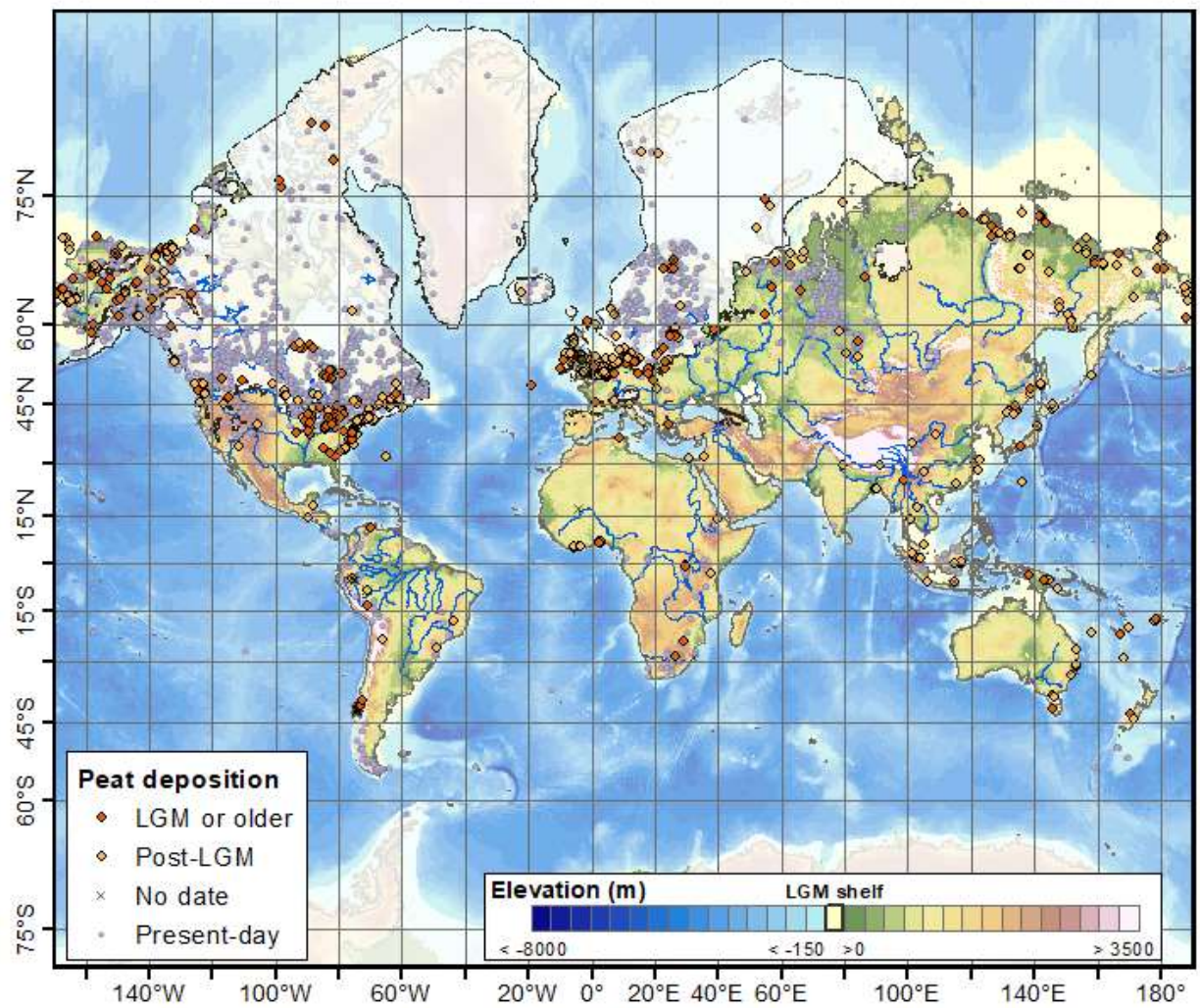


Figure 1.

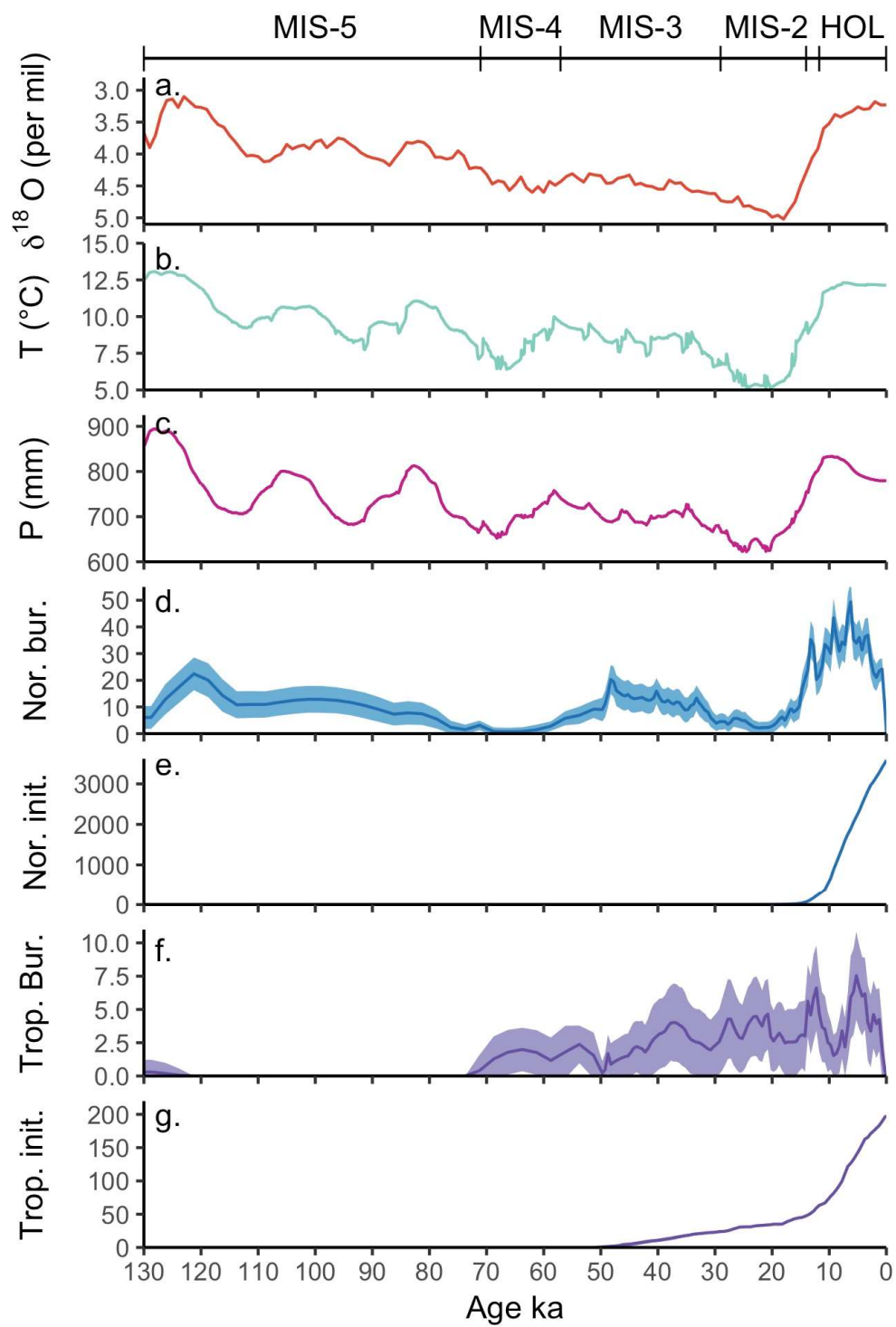


Figure 2.

Table 1. Summary of northern (>40° N) peatland sites and modeled active C stocks between the last interglacial (130 ka) and the LGM (18 ka). Active buried sites indicates the total number of observed sites with active peat accumulation, the median observed peat thickness in the present day (25th & 75th percentile ranges), and the modeled active peatland C stock (error). The correlation between active sites and modeled C stocks was $\rho=0.77$ using Spearman's rank correlation.

Period	Age (ka)	Active buried sites (count)	Thickness (cm)	Modeled active C stock (Pg)
MIS 5e	130-116	45	70 (50-150)	280 (215-405)
MIS 5a-d	116-71	49	75 (50-140)	260 (200-380)
MIS 4	71-57	17	90 (40-340)	210 (160-305)
MIS 3	57 -29	120	100 (40-200)	265 (205-385)
MIS 2	29-21	23	65 (40-100)	135 (105-195)
LGM	21-18	11	25 (20-110)	80 (60-115)

Table 2. Summary of northern and tropical peatland records since the LGM. For both northern and tropical peat sites, the number of now-buried sites with active peat deposition is given (Active buried), as well as the cumulative number and percentage of present-day peatland sites that were established by the period of interest (present-day). Modeled active northern peatland C stocks are also shown and correlated well with total northern peat sites (active buried + present-day; $r = 0.99$); active tropical peatland C stocks are shown in Table S1.

Period	Age	Northern				Tropical		
		Active buried	Present-day	Modeled C stocks		Active buried	Present-day	
	(ka)	(count)	(count)	(%)	(Pg)	(count)	(count)	%
LGM	21-18	11	6	0.2	80 (60-120)	11	37	20
Bølling-Allerød	14.7 – 12.7	84	209	5.8	110 (85-160)	17	57	30
Holocene	11.7	41	328	9.1	140 (110-205)	10	65	33
	8.2	50	1375	38.3	225 (170-325)	5	96	50
Mid-Holocene	5	48	2387	66.6	305 (235-440)	13	146	75
Present-day	2000 CE	0	3586	100	410* (315-590)	0	197	100

*Modeled C stocks are from pre-industrial period (0.1 ka). Since the pre-industrial period, peatland harvesting, drainage, and other land use factors have been observed (25) but are not modeled.